

# Vertical Hole Transport in InAs/InAs<sub>1-x</sub>Sb<sub>x</sub> Type-II Superlattices

**Cheng-Ying Tsai,<sup>1,2</sup> Yang Zhang,<sup>1,2</sup> Zheng Ju,<sup>1,3</sup> and Yong-Hang Zhang<sup>1,2</sup>**  
<sup>1</sup>Center for Photonics Innovation, <sup>2</sup>School of Electrical, Computer and Energy Engineering, <sup>3</sup>Department of Physics, Arizona State University, Tempe, AZ

This abstract reports the study of the vertical hole transport in InAs/InAs<sub>1-x</sub>Sb<sub>x</sub> strained layer type-II superlattice. The low hole mobility in InAs/InAs<sub>1-x</sub>Sb<sub>x</sub> superlattice is considered as the main reason for the low internal quantum efficiency of its mid-wave and long-wave infrared photodetectors, compared with that of its HgCdTe counterparts [1]. Optical measurements using time-resolved photoluminescence (TRPL) and steady-state photoluminescence (SSPL) are implemented to extract the diffusion coefficients and mobilities of holes in the superlattices at various temperatures.

The structure of the samples consists of a mid-wave infrared superlattice (MWSL) absorber region grown atop a long-wave infrared superlattice (LWSL) probe region by using MBE. When the sample is illuminated by laser light, the photogenerated carriers in the MWSL region will diffuse into the LWSL probe region and give photoluminescence, which is used to measure the time of flight of the holes that vertically transport through the entire MWSL region. The hole diffusion coefficients and mobilities in the MWSL can be determined by fitting the TRPL decay profile with the diffusion and rate equations, or by the ratio of the integrated SSPL intensities from LWSL and MWSL [2].

The carrier dynamics in LWSL and MWSL can be described by rate equation and diffusion equation, assuming no external electric field, respectively. The diffusion in the LWSL is negligible due to its thin thickness compared with that of MWSL. The extracted mobilities from SSPL at various temperatures are illustrated in Figure 1, which shows a hole mobility of 56 cm<sup>2</sup>/Vs at 70 K. Besides, the extracted mobility from TRPL fitting (Figure 2) gives a hole mobility of 54 cm<sup>2</sup>/Vs at 70 K, which is in excellent agreement with the result measured by using SSPL.

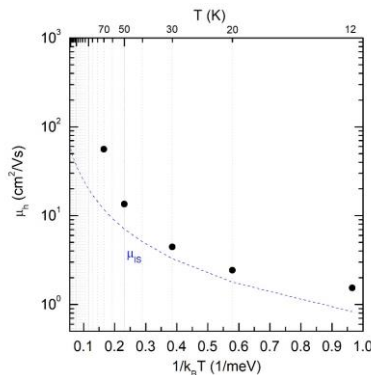


Figure 1. Extracted hole mobilities from SSPL from 12 to 70 K.

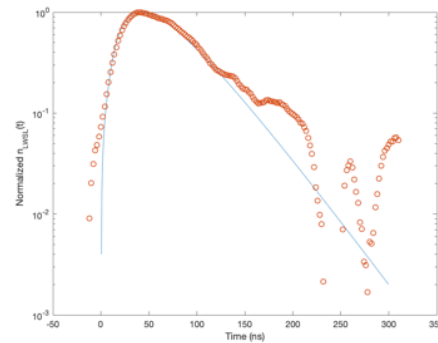


Figure 2. Measured TRPL decay profile (red dots) and theoretical fitting curve (blue line).

- [1] H. S. Kim *et al.*, “Long-wave infrared nBn photodetectors based on InAs/InAsSb type-II superlattices,” *Appl. Phys. Lett.*, vol. 101, p. 161114, 2012.
- [2] T. Amand *et al.*, “Optical detection of vertical transport in GaAs/AlGaAs superlattices: Stationary and dynamical approaches,” *Phys. Rev. B*, vol. 47, no. 12, p. 7155, 1993.

<sup>+</sup> Author for correspondence: [ctsai33@asu.edu](mailto:ctsai33@asu.edu)

## Supplementary Information

The sample structure consists of a 100-nm-thick LWSL and a thick MWSL sandwiched between two 10 nm thick  $\text{In}_{0.9}\text{Ga}_{0.1}\text{As}$  barrier layers. The cross-section of the layer structure and schematic band diagram are shown in Figure 3.

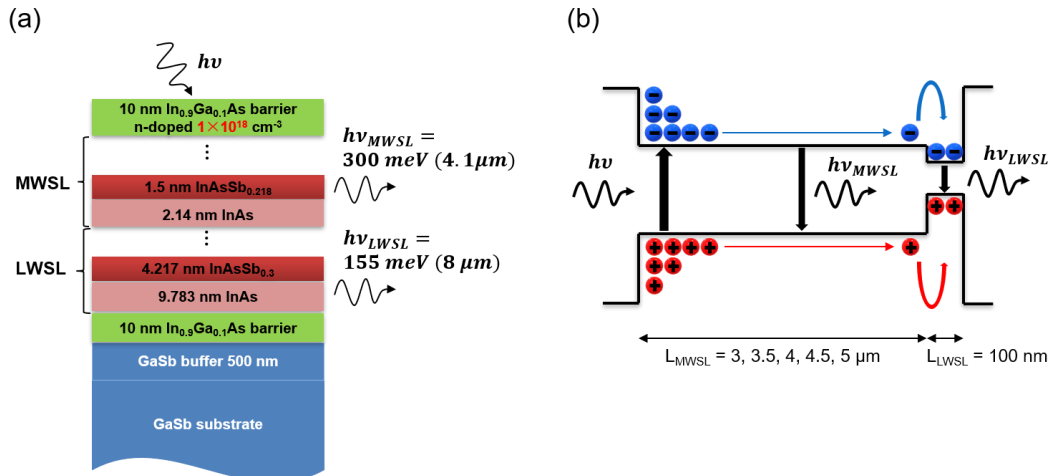


Figure 3. (a) MBE-grown sample structure and (b) schematic band alignment profile for vertical carrier transport study. The MWSL and LWSL are strain-balanced with respect to  $\text{GaSb}$  substrate.

An  $\omega - 2\theta$  XRD (Figure 4) measurement of the sample reveals good crystal quality and an abrupt interface as indicated by Pendellösung fringes. All peaks are well defined and in good agreement with their corresponding layers.

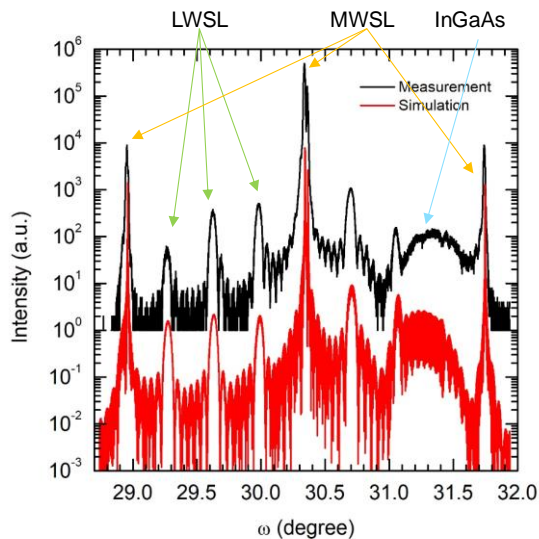


Figure 4.  $\omega - 2\theta$  XRD of the sample for vertical carrier transport study. Black and red lines illustrate the measured and simulated curves, respectively. The peaks for LWSL, MWSL and  $\text{In}_{0.9}\text{Ga}_{0.1}\text{As}$  barrier are as indicated.

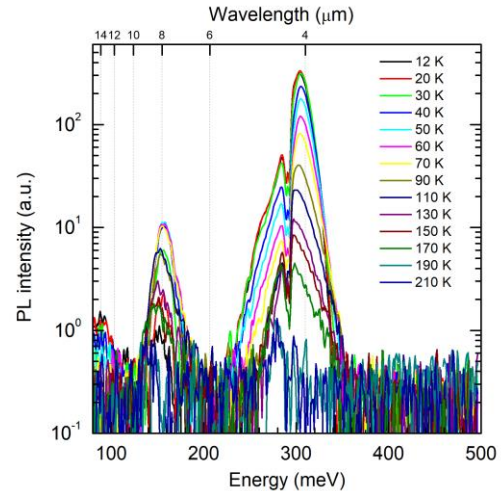


Figure 5. SSPL of the sample taken at various temperatures. Both MWIR and LWIR are observed, indicating carrier diffusion of photogenerated carriers in MWSL into LWSL region.

SSPL of the sample is shown in Figure 5. Two peaks at  $4.1 \mu\text{m}$  (MWIR) and  $8 \mu\text{m}$  (LWIR) are observed. Also, as temperature increases from 12 K to 70 K, the PL intensity of LWIR peak increases one order of magnitude, indicating the photogenerated carriers with higher diffusivity or mobility in the MWSL surface diffuse into LWSL and give PL.

The integrated intensity ratio between  $I_{LWSL}$  and  $I_{MWSL}$  is defined as

$$R = \frac{I_{LWSL}}{I_{MWSL}} = \frac{-\eta_{LWSL} D \left. \frac{dn_{MWSL}(z)}{dz} \right|_{z=L}}{\frac{J_0 \eta_{MWSL}}{1 - L_D^2 \alpha^2} (A L_D (e^{L/L_D} - 1) - B L_D (e^{-L/L_D} - 1) - \alpha^{-1} (e^{-\alpha L} - 1))}, \quad (1)$$

The ratio  $R$  is a function of diffusion coefficient if a constant  $\alpha = 1.5 \times 10^4 \text{ cm}^{-1}$  is applied.

Figure 6(a) illustrates the  $I_{LWSL}$ ,  $I_{MWSL}$ , and  $R$  as a function of temperature taken from SSPL in figure 4 from 12 K to 210 K. The evidence of carrier localization is shown in Figure 6(b) in which the PL peak energy of MWSL increases about 2 meV while the full-width at half-maximum (FWHM) decreases nearly 1 meV from 12 K to 50 K.

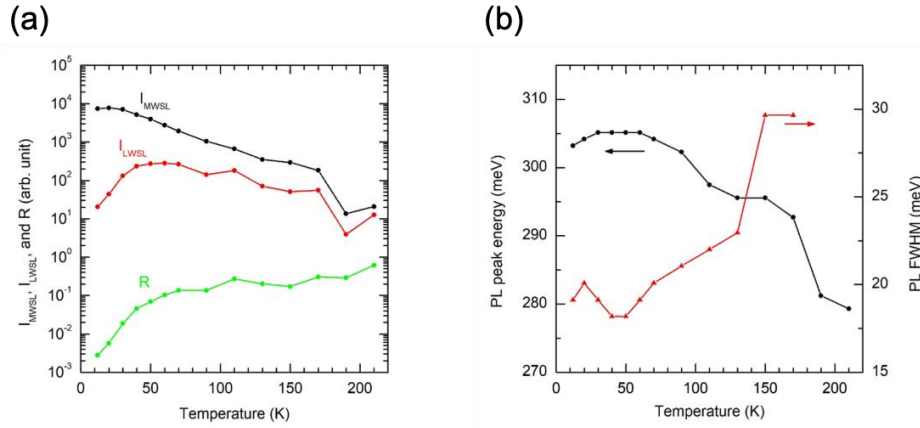


Figure 6. (a)  $I_{LWSL}$ ,  $I_{MWSL}$ , and  $R$  as a function of temperature. The rapid increase of  $R$  as increasing temperature indicates more carriers de-localize in MWSL and diffuse into LWSL. (b) PL peak energy and FWHM as a function of temperature. From 12 K to 50 K, due to carrier delocalization, carriers populate in extended states, resulting in increase in peak energy and decrease in FWHM.

Figure 7 shows the TRPL setup where a long-pass filter with a cut-on wavelength at  $6.5 \mu\text{m}$  is inserted to wipe out the MWIR signal.

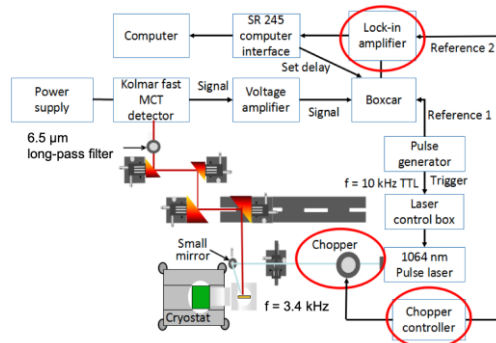


Figure 7. The TRPL signal and its time-delay behavior are measured by a boxcar averager system with a high-speed HgCdTe photodetector at various temperatures using an average pump power of 100 mW from a 1064 nm pulse laser.